Time-Resolved Photoacoustic Calorimetry: Probing the Energetics and Dynamics of Fast Chemical and Biochemical Reactions

KEVIN S. PETERS AND GARY J. SNYDER

Time-resolved photoacoustic calorimetry is a new experimental technique that measures the dynamics of enthalpy changes on the time scale of nanoseconds to microseconds for reactions initiated by absorption of light. When the reaction is carried out in water, it is also possible to obtain the dynamics of the corresponding volume changes. This method has been applied to a variety of biochemical, organic, and organometallic reactions.

ONE PERPLEXING PROBLEM ENCOUNTERED IN DEVELOPing chemical and biochemical reaction mechanisms is establishing the energetics of intervening reactive species. For molecules or molecular complexes with lifetimes shorter than 1 second, it has been exceedingly difficult to obtain direct thermochemical data relating these species to reactants or products. However, with the development of time-resolved photoacoustic calorimetry, it is now feasible to obtain the dynamics of enthalpy changes associated with intervening species having lifetimes as short as 50 ns, provided the reaction of interest can be initiated by the absorption of light.

When a molecule undergoes a chemical transformation in solution, heat is normally released to the solvent and this release gives rise to an increase in temperature; this in turn causes an expansion of the solvent about the reacting molecule. A consequence of this expansion is that an acoustic wave is generated in the medium, and its amplitude is directly related to the amount of heat released in the reaction. Thus, by measuring the amplitude of the acoustic wave it is possible to determine the magnitude of the enthalpy change associated with the decay of the reacting species.

The theory of the photoacoustic effect is well understood and has been discussed in detail by a number of authors (*1–5*). Two experimental methods have evolved that utilize the photoacoustic effect for the determination of reaction energetics. The first method employs a gas microphone and phase-sensitive detection of the acoustic waves produced by absorption of modulated continuous wave light (*6, 7*). The second method, pulsed photoacoustic calorimetry, uses a piezoelectric detector for monitoring the acoustic wave produced upon absorption of light from a pulsed laser (*8–10*). The former method is sensitive to reacting species whose lifetimes are greater than 100 μs whereas the latter method is sensitive to reactions with lifetimes ranging from 50 ns to 20 μs.

The authors are in the Department of Chemistry and Biochemistry, University of Colorado, Boulder, CO 80309-0215.

For pulsed photoacoustic calorimetry two different piezoelectric detectors have been employed. The first is a thin film of poly vinylidene difluoride (PVF_2) that serves as a broadband frequency detector and follows the real-time course of the acoustic wave (*11, 12*). Dynamics and magnitudes of enthalpy changes can be obtained directly by monitoring the acoustic wave as a function of laser beam diameter. A second detector is based on a piezoelectric element composed of lead zirconate–lead titanate (PZT) (*3, 8*). The dynamics of enthalpy changes are obtained by a deconvolution procedure (*9*). In our experiments we have employed PZT detection owning to its greater sensitivity.

In this article we will discuss the design of a photoacoustic calorimeter and the application of pulsed, time-resolved photoacoustic calorimetry to a variety of problems in biochemistry, organic, and organometallic chemistry. In particular we will examine how photoacoustic calorimetry can reveal not only the dynamics of enthalpy changes for ligand dissociation in carboxymyoglobin but also the conformational changes within the protein that accompany the dissociation (*13*). Also, experiments concerning the energetics of diphenyl carbene (*14*) as well as the strain energy in 1-phenyl-*trans*-cyclohexene (*15*) will be presented. Finally, methods for obtaining metal-metal (*16*) and metal-ligand bond enthalpies (*17, 18*) in organometallic complexes will be discussed.

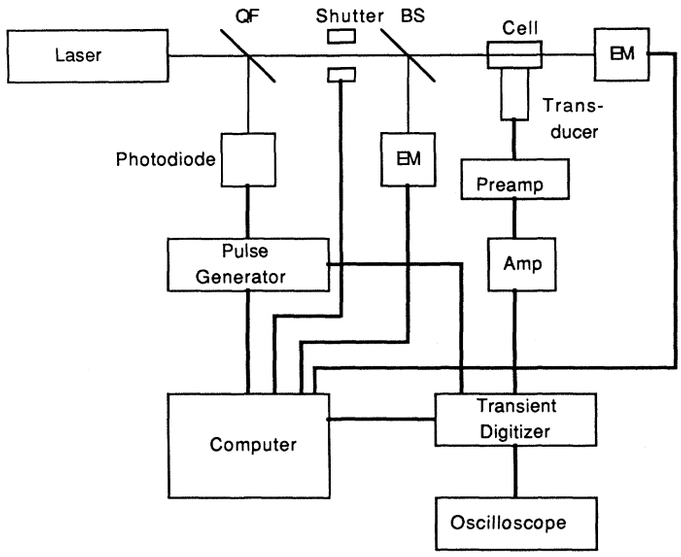

Fig. 1. Schematic representation of the time-resolved photoacoustic calorimetry. Solid lines indicate light path; thick solid lines represent signal paths. Abbreviations: QF, quartz flat; BS, beam splitter; EM, energy meters.

Photoacoustic Calorimeter

The design of our photoacoustic calorimeter is shown in Fig. 1 (*9*). The light source is a nitrogen-pumped dye laser with a pulse width of <1 ns. The light impinging upon the sample varies from 10 to 20 μJ in intensity with a beam diameter of 2 mm. Two energy meters monitor the light intensity before and after the sample, which allows normalization of the photoacoustic signal intensity to the absorbed light energy.

The acoustic wave generated by the photoinitiated event is detected by a piezoelectric element–based transducer clamped to the side of the cuvette. The signal is amplified and recorded by a transient digitizer interfaced to a laboratory computer. The optical densities of the samples normally range from 0.1 to 0.7.

The present apparatus can measure the sum of the enthalpy changes for reactions occurring on a time scale less than 50 ns. For a series of sequential reactions occurring between 50 ns and 20 μs, the dynamics of the enthalpy change for each reaction can be resolved provided they are separated by approximately a decade in time.

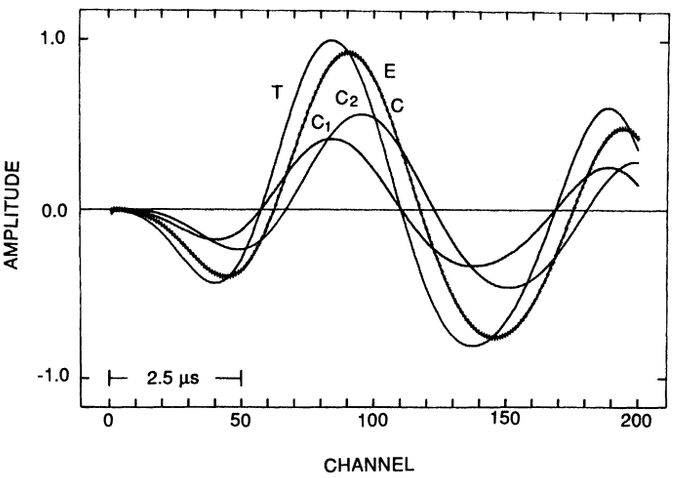

Fig. 2. Photoacoustic waves for sperm whale myoglobin ($8 \times 10^{-5}M$), *p*H 8.0, tris-HCl buffer at 25°C, irradiation at 500 nm. T-wave, deoxymyoglobin used for instrument response function; E-wave (solid line under the hatching), carboxymyoglobin; C_1 and C_2, deconvolution assuming two-step model; C-wave (hatched line) is the sum of C_1 and C_2.

Protein Dynamics

Photoacoustic calorimetry has been applied to a great variety of biochemical problems, which include proton pumping in bacteriorhodopsin (*6*), the photophysics and photochemistry of the plant photosensor pigments phytochrome (*19–21*) and chlorophyll (*22*), and carbon monoxide dissociation in myoglobin (*13, 23*).

For the binding of a ligand to the oxygen transport protein myoglobin there are two central questions that are yet to be answered: the pathway by which a ligand diffuses from the heme binding site to the solvent and the means by which the protein structure modulates the binding energy of the ligand. From the initial x-ray structure studies of deoxymyoglobin and carboxymyoglobin (*24, 25*) it was immediately apparent that there are no direct channels between the solvent and the heme pocket through which the ligand may diffuse. In order to create a channel for ligand diffusion molecular dynamics calculations (*26*) reveal that large amplitude motions of many amino acid side chains must occur. However, these molecular dynamics studies were not able to define a unique pathway for ligand diffusion.

Myoglobin (Mb) has been the subject of several laser flash photolysis studies. Upon absorption of light, the excited state of carboxymyoglobin $(MbCO)^*$ decays in 350 femtoseconds (fs), breaking the Fe^{2+}–CO bond, to form a geminate pair (Mb:CO) where the CO is thought to be within the heme pocket (*27*). On the time scale of 180 ns, the geminate pair relaxes to produce deoxymyoglobin and free carbon monoxide (Mb + CO) (*28*) with a quantum yield of 0.96 at 22° C.

$$\text{MbCO} \xrightarrow{h\nu} (\text{MbCO})^* \xrightarrow{350\ \text{fs}} \text{Mb:CO} \xrightarrow{180\ \text{ns}} \text{Mb} + \text{CO} \quad (1)$$

From gas-liquid microcalorimetry (*29*), the overall binding of CO to sperm whale deoxymyoglobin (Mb + CO → MbCO) is exothermic by 17.7 ± 0.4 kcal/mole at *p*H 8.0 in 0.1*M* tris-HCl buffer. The energetics of intermediate states, including the geminate pair, have not been determined.

In a study of the photodissociation of CO from sperm whale carboxymyoglobin there are two potential mechanisms for the generation of acoustic waves. The first is expansion of the solvent, owing to heating resulting from the release of energy to the solution by the reacting molecules. For carboxymyoglobin, heat is liberated both by the relaxation of the excited state to form the geminate pair and by the relaxation of the geminate pair to produce deoxymyoglobin and CO. The second potential source of acoustic waves is conformational changes within the protein to create a channel for ligand diffusion. These conformational changes may lead either to an increase or a decrease in the volume of the protein, thereby producing acoustic waves. Thus the overall volume change that generates the acoustic wave will have contributions from both thermal (V_{th}) and conformational components (V_{con}).

$$\Delta V = \Delta V_{th} + \Delta V_{con} \quad (2)$$

The thermal component of the volume change, ΔV_{th}, will be related to the change in temperature, ΔT, through the thermal expansion coefficient of the solvent, β, and the initial volume of the irradiated system, V_0.

$$\Delta V_{th} = \beta V_0 \Delta T \quad (3)$$

The two contributions to the observed acoustic wave, produced by ΔV, can be separated from one another by studying the temperature dependence of the observed acoustic wave. The thermal expansion coefficient, β, for water (and buffered water) is temperature-dependent, whereas to a first approximation the volume change caused by conformational changes within the protein should be independent of temperature over a narrow range. By examining the temperature dependence of the acoustic wave, the thermal and conformational components may be separated.

For a photoacoustic calorimeter that uses PZT detection of the acoustic wave, the observed voltage from the transducer [$E(t)$] will be the result of the convolution of a time-dependent heat source, $H(t)$, with the instrument response function, $T(t)$ (*9*);

$$E(t) = H(t) * T(t) \quad (4)$$

To obtain the dynamics of the enthalpy and volume changes, it is necessary to develop a kinetic model for $H(t)$ that has parameters accounting for rates of the heat depositions as well as the amplitudes of the volume changes. For the photodissociation of carboxymyoglobin we assumed (*13*) that a two-step process gives rise to the observed experimental wave $E(t)$: on a time scale of less than 50 ns the formation of the geminate pair from the excited state of carboxymyoglobin will occur, and on a time scale longer than 100 ns there will be a release of CO to the solvent. To obtain $H(t)$ it is necessary to measure the instrument response function $T(t)$, which reflects the response of the transducer to a pressure wave whose

duration is shorter than the response time of the transducer, 50 ns. This entails the use of a calibration compound that converts the entire energy of the photon into heat in less than 50 ns and undergoes no photochemistry on this time scale. The instrument response function, $T(t)$, in the myoglobin study is obtained by the irradiation of deoxymyoglobin. Kinetic and thermodynamic information for carboxymyoglobin is then obtained by adjusting a set of parameters to generate $H(t)$, which is then convoluted with $T(t)$ to produce a calculated voltage, $C(t)$. The two time-dependent voltages $C(t)$ and $E(t)$ are then compared and the parameters are optimized to minimize their difference.

An example of such a deconvolution of an acoustic wave for carboxymyoglobin, irradiated at 500 nm in a *p*H 8.0 tris-HCl buffer at 25°C, is shown in Fig. 2. The acoustic wave from carboxymyoglobin, that is, the *E*-wave, is found to be shifted with respect to the instrument response function produced from deoxymyoglobin, the *T*-wave. The shift in the *E*-wave reveals that there are kinetic processes occurring on the time scale of the instrument response. Assuming a two-step model for the dissociation, the deconvolution produces two acoustic waves, C_1 and C_2, whose sum closely reproduces the observed acoustic wave for MbCO. By studying the temperature dependence of C_1 and C_2 it is then possible to separate the dynamics of enthalpy and volume changes for the two processes (*13*). The results are shown in Fig. 3.

The overall enthalpy change, $\Delta H = 14.6 \pm 3.4$ kcal/mole, for the dissociation of CO from ground-state carboxymyoglobin to form deoxymyoglobin and solvated CO is in good agreement with the value determined by microcalorimetry ($\Delta H = 17.7 \pm 0.4$ kcal/mole). The most surprising finding is that the formation of the geminate pair is exothermic by 2.2 ± 2.8 kcal/mole and is accompanied by a negative volume change, $\Delta V = -10.0 \pm 1.0$ ml/mole. Furthermore, relaxation of the geminate pair to give Mb + CO is an endothermic process. It has recently been proposed (*30*), on the basis of x-ray structural studies of metmyoglobin (Fe^{+3}) where the heme iron is covalently bound to a phenyl group, that the pathway for ligand diffusion involves the breaking of a salt bridge formed between arginine-45 and the propionate side chain of the heme group. The breaking of a salt bridge and accompanying solvation of the resulting two charges will cause electrostriction of the water and in turn lead to a negative volume change for the system. For the second step, which is spontaneous yet endothermic, there must be a substantial increase in entropy ($T\Delta S > 16.8$ kcal/mole) accompanying re-formation of the salt bridge.

Photoacoustic calorimetry has the potential to yield short-time enthalpic and volume change information for a number of biochemical processes providing the reactions can be light-initiated. The visual pigment rhodopsin, the proton and chloride pumps bacteriorhodopsin and halorhodopsin, as well as photosynthetic units are obvious candidates for investigation. It is important to note, however, that enthalpic and volume changes are obtained from $H(t)$. To construct $H(t)$, a kinetic model for the processes of interest must be assumed which in most instances will rely upon prior kinetic and quantum yield studies.

Organic Reaction Intermediates

Photoacoustic calorimetry has been employed in a variety of investigations of organic reaction intermediates. The studies concern the energetics of the radical pair formed in the reaction of triplet benzophenone with aniline (*8*), the reactions of carbenes (*14*), the strain energy of 1-phenyl-*trans*-cyclohexene (*15*), the energetics of biradicals (*9*), solvent effects upon ion pairs (*31*), the bond enthalpies of Si–H (*32*) and Sn–H (*33*), the dynamics of the reaction of iodide with the triplet state of benzophenone (*12*), the energies of alkene relaxed triplet states (*34*), and energy storage in the spiro[1,8-*a*]dihydroindolizine-betaine system (*35*). To illustrate the versatility of the technique, the photoacoustic calorimetric investigations of the strain energy of 1-phenyl-*trans*-cyclohexene and carbene reactions will be presented.

The concept of strain energy in organic compounds has long fascinated chemists. Numerous studies of a variety of organic molecules have been directed toward quantifying strain energy. However, for torsional strain about double bonds in cyclic systems there is little information relating strain energy with ring size. Recently, several groups have reported (*36, 37*) that upon triplet sensitization of 1-phenyl-*cis*-cyclohexene by benzophenone (τ_1) that 1-phenyl-*trans*-cyclohexene is produced from the triplet state (T_1) of 1-phenyl-*cis*-cyclohexene in 65 ns (τ_2) with a quantum yield of 0.36 and decays in 9 μs (τ_3) to reform 1-phenyl-*cis*-cyclohexene (Fig. 4).

Our photoacoustic studies (*15*) of the benzophenone-sensitized isomerization of 1-phenyl-*cis*-cyclohexene revealed that, in order to properly deconvolute the photoacoustic wave, three sequential decay processes must be assumed. The kinetics for formation τ_1 (<10 ns) and decay τ_2 (64 ± 7 ns) of the triplet state, and the isomerization of the *trans* alkene τ_3 (9.7 ± 2.0 μs) are in excellent agreement with laser flash photolysis studies (*36, 37*). The 1-phenyl-*trans*-cyclohexene strain energy, defined as the enthalpy difference between 1-phenyl-*cis*-cyclohexene and 1-phenyl-*trans*-cyclohexene, is 44.7 ± 5.0 kcal/mole. The energy of the triplet state of 1-phenyl-*cis*-cyclohexene is 56.0 ± 3.4 kcal/mole. This is the first direct measurement of the energy of a relaxed triplet of an alkene. Recently an investigation of the energetics and dynamics of a number of substituted alkene and diene triplet states has appeared (*34*).

The chemistry of carbene reactions has been thoroughly investigated and yet there are many important questions that have not been fully answered. One of the major problems is the lack of thermochemical data for carbenes and their reactions.

The photolysis of diphenyldiazomethane to produce triplet diphenylcarbene and the reaction of the triplet carbene with molecular oxygen have been studied with photoacoustic calorimetry (*14*).

$$Ph_2CN_2 \xrightarrow{h\nu} {}^3Ph_2C: + N_2 \xrightarrow{O_2} Ph_2COO \qquad (5)$$

In benzene, the enthalpy change for the formation of triplet diphenylcarbene from diphenyldiazomethane is $\Delta H = 0 \pm 1.7$ kcal/mole. The subsequent reaction of the triplet carbene with oxygen is found to be highly exothermic $\Delta H = -34.7 \pm 2.4$ kcal/mole.

One potential problem for reactions that involve dissociation is the contribution to the acoustic wave from the attendant increase in volume for the reaction. In the myoglobin study, the volume

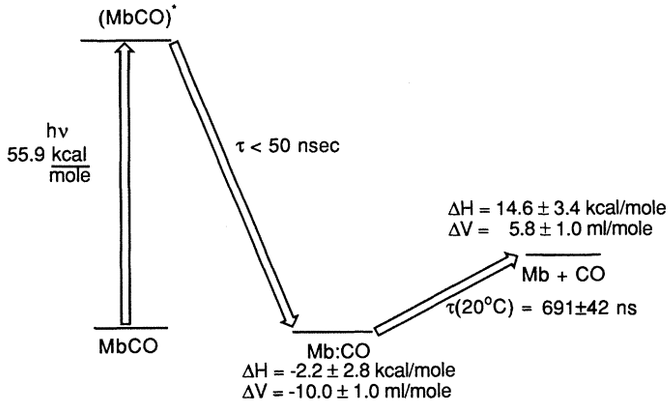

Fig. 3. Reaction enthalpy and volume change profile for the photodissociation of sperm whale carboxymyoglobin at *p*H 8.0, tris-HCl buffer at 20°C.

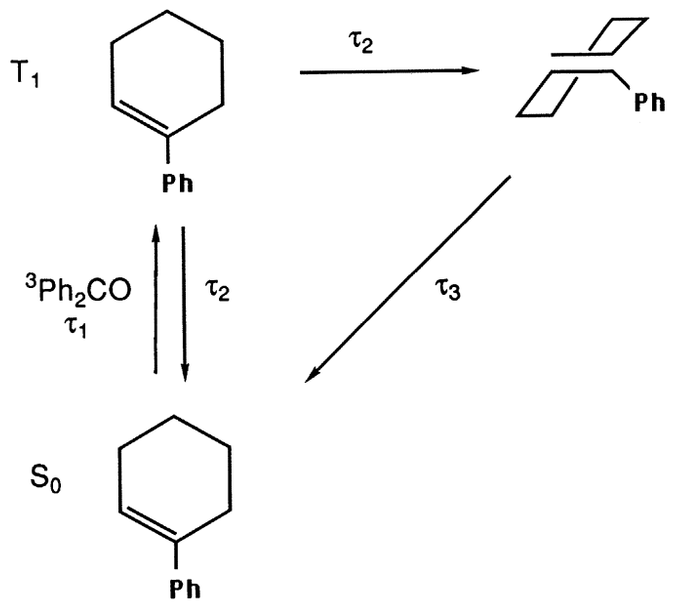

Fig. 4. Reaction scheme for the benzophenone triplet sensitized isomerization of 1-phenyl-*cis*-cyclohexene to 1-phenyl-*trans*-cyclohexene.

changes made a major contribution to the overall acoustic wave. Unfortunately for reactions in organic solvents it is not practical to separate the thermal component from the volume component through the temperature dependence of the acoustic wave. Although the thermal expansion coefficient for water is highly temperature dependent, those for organic solvents are much less so. Since the thermal expansion coefficients for organic solvents are much larger and their heat capacities are much smaller than the corresponding parameters for water, the enthalpy contribution to the acoustic wave will be greater. One possible approach to separating the thermal and volume contributions is to examine the reaction of interest in a variety of solvents with differing thermal expansion coefficients. If volume changes are contributing significantly to the acoustic wave, then comparison of the acoustic wave amplitude of a reference compound, which does not have a volume change associated with its photochemistry, with that of the system of interest should reveal the relative contribution of the volume change to the photoacoustic signal. At present, the value for the reaction enthalpy of diphenyldiazomethane to diphenylcarbene must be regarded as a lower limit.

Organometallic Compounds

The enthalpies of metal-metal and metal-ligand bonds are very important quantities for the development of an understanding of reactivity and selectivity in organometallic chemistry. However examination of the thermochemical literature reveals that very few metal-metal and metal-ligand bond enthalpies are known. Time-resolved photoacoustic calorimetry is beginning to provide new thermochemical data for organometallic compounds. The potential of the technique will be illustrated by discussing recent experiments on the metal-ligand bond enthalpy in L-$Cr(CO)_5$, where L is the ligand (*17*), the metal-hydrogen bond enthalpy in $(\eta^5\text{-}C_5Me_5)(PMe_3)IrH_2$ (*18*), and the metal-metal bond enthalpy in $(CO)_5Mn\text{-}Mn(CO)_5$ (*16*).

The metal-ligand bond enthalpy in L-$Cr(CO)_5$ has been measured for many common ligands by photoacoustic calorimetry (*17*). $Cr(CO)_6$ is known to undergo ligand substitution reactions upon photolysis. Laser flash photolysis studies have shown that upon absorption of a photon the excited state decomposes in less than 25 ps (*38*) by CO loss to give $Cr(CO)_5$, which is coordinated to the solvent. In the presence of a ligand, L, replacement of the solvent by L will take place with a pseudo–first-order rate constant, k.

$$Cr(CO)_6 \xrightarrow[\text{heptane}]{h\nu} Cr(CO)_5(\text{heptane}) \xrightarrow{k[L]} Cr(CO)_5L \qquad (6)$$

The observed acoustic wave will have two contributions: dissociation of CO followed by coordination of heptane, and the replacement of the solvent by the ligand. The first process will occur on a time scale faster than the instrument response function, < 50 ns. The rate of the second process depends on the concentration of L, and can be varied so that this process occurs within the response time of the transducer (50 ns to 20 μs).

A list of the enthalpy changes for the ligand replacement reactions and the associated kinetics is available (*17*). The enthalpy changes are found to vary from 5.4 kcal/mole for the replacement of CO by $P(n\text{Bu})_3$ to 17.4 kcal/mole for the replacement of CO by tetramethylethylene. Interestingly, the enthalpy change associated with the replacement of CO by a solvent molecule, heptane, is 27.0 kcal/mole. Given that the CO bond dissociation enthalpy for $Cr(CO)_6$ in the gas phase is 36.8 kcal/mole (*39*), the coordination enthalpy of the solvent with $Cr(CO)_5$ is 9.8 kcal/mole.

The metal-metal bond enthalpy of $Mn_2(CO)_{10}$ has been the subject of numerous investigations. The values are found to range from 16 kcal/mole to 41 kcal/mole (*16*). This range of values illustrates the difficulty in obtaining specific bond enthalpies for organometallic compounds. The photolysis of $Mn_2(CO)_{10}$ proceeds by two pathways: metal-ligand bond cleavage to produce $Mn_2(CO)_9$ and metal-metal bond cleavage to produce $Mn(CO)_5$. Since the quantum yields for both of these processes as well as the Mn–CO bond enthalpy are known, it is possible to obtain the Mn–Mn bond enthalpy directly from photoacoustic calorimetry (*16*). This value is found to be 38 ± 5 kcal/mole. Most of the error in the measurement reflects the uncertainty in the quantum yield data.

The reactivity of the metal-hydrogen bond is fundamentally important in many organometallic reactions, yet very few metal-hydrogen bond enthalpies are known. One general approach toward obtaining these thermochemical data relies upon the hydrogen abstraction by *tert*-butoxy radical.

$$(L)_nM\text{-}H + t\text{-}BuO\cdot \rightarrow (L)_nM\cdot + t\text{-}BuOH \qquad (7)$$

The M–H bond enthalpy can be deduced by measuring the enthalpy change for the reaction and subtracting the O–H bond enthalpy of *t*-butanol. By means of the photolysis of *tert*-butyl peroxide to generate the radical, the Ir–H bond enthalpy in $(\eta^5\text{-}C_5Me_5)(PMe_3)IrH_2$ was determined to be 72.9 ± 4.3 kcal/mole (*18*). This value is in excellent agreement with a value of 74 kcal/mole estimated from thermochemical and kinetic data (*18*), thus substantiating the validity of the technique. The use of *t*-butoxy radical as a hydrogen atom abstractor should be generally applicable for determining metal-hydrogen bond enthalpies.

Conclusions

Although pulsed time-resolved photoacoustic calorimetry is still in its early stages of development, it has already manifested itself as a powerful method for gaining insights into dynamics of enthalpy and volume changes for both ground- and excited-state species. There is a need, however, for careful interpretation of the photoacoustic data, particularly in regard to volume changes. For reactions in

water, the problem is directly approached through temperature dependence studies. For reactions in organic solvent, there must be further investigations into the magnitude of the effect.

In the foreseeable future time-resolved photoacoustic calorimetry will be extended onto the 1-ns time scale, given the recent developments in piezoelectric transducers and transient-recording devices. The technique should find wide ranging application to problems in chemistry and biochemistry that include solid-state reactions and dynamics of proteins in membranes.

REFERENCES AND NOTES

1. A. G. Bell, *Philos. Mag.* **11**, 510 (1881).
2. W. R. Harshbarger and M. B. Robin, *Acc. Chem. Res.* **6**, 329 (1973).
3. C. K. N. Patel and A. C. Tam, *Rev. Mod. Phys.* **53**, 517 (1981).
4. A. C. Tam, *ibid.* **58**, 381 (1986).
5. M. W. Sigrist, *J. Appl. Phys.* **60**, R83 (1986).
6. D. R. Ort and W. W. Parsons, *Biophys. J.* **25**, 355 (1979).
7. T. A. Moore, D. Benin, R. Tom, *J. Am. Chem. Soc.* **104**, 7356 (1982).
8. L. J. Rothberg, J. D. Simon, M. Bernstein, K. S. Peters, *ibid.* **105**, 3464 (1983).
9. J. E. Rudzki, J. L. Goodman, K. S. Peters, *ibid.* **107**, 7849 (1985).
10. S. E. Braslavsky, in *Primary Photo-Processes in Biology and Medicine*, R. V. Bensasson, G. Jori, E. J. Land, Eds. (Plenum, New York, 1985), pp. 147–158.
11. S. J. Komorowski and E. M. Eyring, *J. Appl. Phys.* **62**, 3066 (1987).
12. K. Heihoff and S. E. Braslavsky, *Chem. Phys. Lett.* **131**, 183 (1986).
13. J. A. Westrick, J. L. Goodman, K. S. Peters, *Biochemistry* **26**, 8313 (1987).
14. K. S. Peters, in *Kinetics and Spectroscopy of Carbenes and Biradicals*, M. Platz, Ed. (Plenum, New York, in press).
15. J. L. Goodman, K. S. Peters, H. Misawa, R. A. Caldwell, *J. Am. Chem. Soc.* **108**, 6803 (1986).
16. J. L. Goodman, K. S. Peters, V. Vaida, *Organometallics* **5**, 815 (1986).
17. G. K. Yang, K. S. Peters, V. Vaida, *Chem. Phys. Lett.* **125**, 566 (1986).
18. S. P. Nolan, *et al.*, *J. Am. Chem. Soc.* **109**, 3143 (1987).
19. K. Heihoff, S. E. Braslavsky, K. Schaffner, *Biochemistry* **26**, 1422 (1987).
20. S. E. Braslavsky, *Pure Appl. Chem.* **56**, 1153 (1984).
21. M. Jabben, K. Heihoff, S. E. Braslavsky, K. Schaffner, *Photochem. Photobiol.* **40**, 361 (1984).
22. M. Jabben *et al.*, *ibid.* **43**, 127 (1986).
23. W. P. Leung, K. C. Cho, S. K. Chau, C. L. Choy, *Chem. Phys. Lett.* **141**, 220 (1987).
24. J. C. Kendrew *et al.*, *Nature* **185**, 422 (1960).
25. T. Takano, *J. Mol. Biol.* **110**, 569 (1977).
26. D. A. Case and M. Karplus, *ibid.* **132**, 343 (1979).
27. J. L. Martin *et al.*, *Proc. Natl. Acad. Sci. U.S.A.* **80**, 173 (1983).
28. E. R. Henry, J. H. Sommer, J. Hofrichter, W. Eaton, *J. Mol. Biol.* **166**, 443 (1983).
29. S. A. Rudolph, S. O. Boyle, D. F. Dresden, S. J. Gill, *Biochemistry* **11**, 1098 (1972).
30. D. Ringe, G. A. Petsko, D. E. Kerr, P. R. Ortiz de Montellano, *ibid.* **23**, 2 (1984).
31. J. L. Goodman and K. S. Peters, *J. Am. Chem. Soc.* **108**, 1700 (1986).
32. J. M. Kanabus-Kaminska, J. A. Hawari, D. Griller, C. Chatgiliarloglu, *ibid.* **109**, 5267 (1987).
33. T. J. Burkey, M. Majewski, D. Griller, *ibid.* **108**, 2218 (1986).
34. J. A. Lavilla and J. L. Goodman, *Chem. Phys. Lett.* **141**, 149 (1987).
35. N. A. Garcia, G. Rossbroich, S. E. Braslavsky, H. Durr, C. Dorweiler, *J. Photochem.* **31**, 297 (1985).
36. R. Bonneau, *ibid.* **10**, 439 (1979).
37. R. A. Caldwell and C. V. Cao, *J. Am. Chem. Soc.* **104**, 6174 (1982).
38. J. A. Welch, K. S. Peters, V. Vaida, *J. Phys. Chem.* **86**, 1941 (1982).
39. K. E. Lewis, D. M. Golden, G. P. Smith, *J. Am. Chem. Soc.* **106**, 3905 (1984).

40. This work has been supported by grants from the National Science Foundation and the National Institute of Health.

Heterologous Expression of Excitability Proteins: Route to More Specific Drugs?

HENRY A. LESTER

Many clinically important drugs act on the intrinsic membrane proteins (ion channels, receptors, and ion pumps) that control cell excitability. A major goal of pharmacology has been to develop drugs that are more specific for a particular subtype of excitability molecule. DNA cloning has revealed that many excitability proteins are encoded by multigene families and that the diversity of previously recognized pharmacological subtypes is matched, and probably surpassed, by the diversity of messenger RNAs that encode excitability molecules. In general, the diverse subtypes retain their properties when the excitability proteins are expressed in foreign cells such as oocytes and mammalian cell lines. Such heterologous expression may therefore become a tool for testing drugs against specific subtypes. In a systematic research program to exploit this possibility, major considerations include alternative processing of messenger RNA for excitability proteins, coupling to second-messenger systems, and expression of enough protein to provide material for structural studies.

The author is in the Divison of Biology, California Institute of Technology, Pasadena, CA 91125.

MANY DRUGS IN THE MODERN PHARMACOPOEIA ACT ON ion channels, receptors, and ion pumps in biological membranes. These molecules belong to several families of intrinsic membrane proteins that I term collectively "excitability proteins." Two facts help to explain the medical importance of drug effects on excitability proteins. (i) Because excitability proteins function at the cell surface, they are accessible to drugs present in the extracellular fluid. (ii) Because these proteins usually control cellular events that operate on a time scale of milliseconds to minutes, their activation or inhibition can often be rapidly monitored by the physician and readily appreciated by the patient.

The available drugs, despite their utility, have many side effects. This article concerns a particular type of side effect that seems to arise because many excitability proteins are members of multigene families: there are undesired interactions with homologous excitability proteins in tissues or cells that are not the drug's intended target.

I cite here a few examples of such side effects. These examples are chosen because their protein targets span the known classes of excitability molecules.

1) The β-adrenergic receptor blockers, such as propranolol, are effective antihypertensive agents because of their actions on the cardiovascular system. However, they may cause fatigue, depression, and other effects related to actions on β-adrenergic receptors in the central nervous system.